Desalination and Water Treatment
www.deswater.com

doi: 10.5004/dwt.2020.24803

173 (2020) 274–282
January

Elimination of Ni(II) from water samples using composite of magnetic nanoparticles orange peel (MNP-OP)

Mansoor Khan[a,*], Jasmin Shah[b], Muhammad Rasul Jan[b]

[a]*Department of Chemistry, Kohat University of Science and Technology, Khyber Pakhtunkhwa, Pakistan, Tel./Fax: +92-91-9216652; email: mansoor009988@gmail.com*
[b]*Institute of Chemical Sciences, University of Peshawar, Khyber Pakhtunkhwa, Pakistan*

Received 8 April 2019; Accepted 21 August 2019

ABSTRACT

Orange peel powder was impregnated with magnetic nanoparticles through co-precipitation with Fe_3O_4 nanoparticles and used for the removal of Ni(II) from aqueous solutions. The adsorbent magnetic nanoparticles orange peel powder (MNP-OPP) was characterized by Fourier-transform infrared spectroscopy for surface functional group and scanning electron microscope for the surface morphology. The effectiveness of Ni(II) removal was studied systematically as a function of solution pH 2–7, amount of adsorbent 20–220 mg, contact time 20–60 min, initial metal ion concentration 200–120 mg L^{-1} and temperature 303–363 K. Maximum uptake of Ni(II) (98.12%) was observed at pH 7 with 60 min agitation time. The kinetic studies showed that the data followed second-order kinetics with a correlation coefficient of 0.9948. Adsorption isotherms show that the data fitted to Langmuir adsorption isotherm (R^2 = 0.9954) with the monolayer adsorption capacity (Q_0) of 110.12 mg g^{-1}. The thermodynamic study revealed that the adsorption of Ni(II) ions onto the MNP-OPP composite was spontaneous and endothermic. The effect of different coexisting ions like alkali, alkaline earth metals and transition metals was studied and the results revealed that orange peel with magnetic nanoparticle composite can be used for removal of Ni(II) from water samples as an alternative adsorbent. The method was successfully applied to real environmental water like tap water, canal water and river water with quantitative % adsorption results.

Keywords: Adsorption; Impregnated orange peel; Magnetic nanoparticles; Nickel; Heavy metals

1. Introduction

Toxic heavy metals mentioned by World Health Organization include lead Pb(II), Cd(II), Zn(II), Ni(II), Co(II), Cu(II) and Hg(II) [1]. These heavy metals cause severe health problems in the central nervous system, reproductive system and immune system of human beings [2]. Among these heavy metals nickel is the 24th abundant element in the earth's crust, used in storage batteries, steel manufacturing, electroplating and dyeing industries [3]. Nickel is useful at trace amount because it activates some enzymatic activity like urease, discovered by Zerner in 1975 [1]. The amount of nickel greater than permissible levels causes skin dermatitis, renal edema, and lung cancer. Therefore the removal of nickel to permissible limits from natural water is an important task [3,4].

Methods reported for heavy metals removal include ion exchange, solvent extraction, reverse osmosis, electrodialysis precipitation, flocculation and membrane separation [5,6]. These methods have disadvantages such as high running cost, toxic chemical sludge, and high capital investment; also the methods are not environmentally friendly. Therefore, environmental friendly technologies are required to bring the concentration of heavy metals to the permissible level [7].

* Corresponding author.

Among the separation methods, adsorption is commonly used for the removal of heavy metals from water samples. It has advantages over the other methods due to its low cost, availability of adsorbent and removal of heavy metals from aqueous solutions to very low concentrations [3]. Various kinds of adsorbents were used such as mesoporous silica, zeolites, biomass, and biopolymers [8].

Biosorbent is a type of adsorbent derived from biological material like agriculture waste, forest waste, and algae, etc. In recent years, different low cost and easily available biosorbent like waste tea leaves [3] pine bark [9], sawdust [10], peat biomass [11], algae [12], fly ash [13], yeast biomass [14], almond husk [15], carbonized sawdust [16], and seaweed waste [17] was employed for the removal of Ni(II) from water samples. Orange peels consist of cellulose having hydroxyl and carbonyl functional group, which are the active sites for binding the heavy metals.

Advancement of the nanotechnology is important due to its widespread application in different fields like mineral separation, catalysis, magnetic refrigerating system, magnetic storage devices, heat transfer application in drug delivery system, magnetic resonance imaging and cancer therapy [18,19]. Magnetic nanoparticles (MNP) have a large surface area, magnetic properties, a large number of active sites for metals, exhibits good adsorption efficiency and can be used as an adsorbent for the removal of heavy metals [1]. The methods such as hydrothermal synthesis [20], thermal decomposition [21], the sol-gel method [22], colloidal chemistry method [23] and co-precipitation method [24] are used for the synthesis of MNP.

The present work aimed to prepare a composite of waste orange peel with magnetic nanoparticle (MNP-OP). Orange peel contains pectin, lignin, cellulose, and hemicellulose, rich in hydroxyl and carboxyl groups, while the MNP possesses merits of high surface area and separation convenience with an external magnet. Therefore, the combined effect of functional groups of orange peel and the high surface of MNP in MNP-OP composite adsorbent was evaluated for the removal of Ni(II) ions in the batch method from aqueous solution.

2. Experimental setup

2.1. Chemicals

All chemicals used were of analytical reagent grade or similar purity and used without further purification. Standard solutions of Ni(II) were prepared by diluting the stock solution (1,000 mg L^{-1}) purchased from E. Merck Company (Darmstadt, Germany). Ferric chloride hexahydrate ($FeCl_3{\cdot}6H_2O$), and ferrous sulfate heptahydrate ($FeSO_4{\cdot}7H_2O$), supplied by BDH laboratories, BH15 ITD Poole, England. Ammonia solution (35%), hydrochloric acid (37%), sodium hydroxide, boric acid, phosphoric acid, and acetic acid were supplied by Sigma-Aldrich (St. Louis, MO, USA).

2.2. Instrumentation

A Perkin-Elmer flame atomic absorption spectrometer Model AA 200 Perkin Elmer (CA, USA) with air–acetylene flame having 10 cm long-slot burner head was used for absorbance measurements. The hollow cathode lamps were used as radiation sources with the working condition as prescribed by the manufacturer.

The surface morphology of the prepared MNP-OP was analyzed by scanning electron microscopy (SEM) using JSM5910 (JEOL, Tokyo, Japan). The specimens for SEM analysis were prepared by coating the samples as a thin layer with double adhesive carbon tape over aluminum stubs. The functional groups in the surface of orange peels (OP) and MNP-OP composite were confirmed from the infrared spectrum analyzed by IR Prestige– 21 SHIMADZU (Tokyo, Japan).

The N_2 adsorption/desorption was carried out on a Surface Area Analyzer, NOVA2200e Quantachrome, USA at 77.4 K. The samples were outgassed before analysis at 100°C for 2 h using high vacuum line to remove all the adsorbed moisture or gases from the adsorbent surface and pores. The surface area of the sample was calculated using both the Brunauer–Emmett–Teller (BET) and Barrett–Joyner–Halenda (BJH) method, the pore volume was calculated from the adsorbed nitrogen after complete pore condensation (P/P_0 = 0.995) using the ratio of the densities of liquid and gaseous nitrogen. The pore size and pore volume were calculated using the BJH method.

2.3. Adsorbent preparation

OP from juice shops and local markets were collected. For the removal of dirt particles, the orange peel was washed with distilled water, dried and ground. The crushed orange peels were passed through a sieve and obtained uniform particle size <355 μm.

The chemical precipitation method is one of the most reliable methods used for the preparation of MNP [19]. Fe(II) and Fe(III) were mixed in a 1:2 ratio in basic media for co-precipitation. For this purpose, 6.3 g of $FeCl_3{\cdot}6H_2O$ and 4.2 g $FeSO_4{\cdot}7H_2O$ were dissolved in 200 mL of distilled water with vigorous stirring under the nitrogen atmosphere. The solution was kept at 80°C; black precipitate of Fe_3O_4 was obtained when 20 mL of 25% ammonia solution was added. For the composite preparation of Fe_3O_4 with orange peel, 10 g of OP was added to the solution at 80°C for 60 min under vigorous stirring. The resultant Fe_3O_4-OP was filtered, washed with distilled water and dried in an oven at 100°C. The Fe_3O_4-OP composite obtained was checked for its magnetic property with a magnetic rod, it was observed that adsorbent was attracted towards the magnetic rod.

2.4. Batch adsorption studies

Adsorption behavior of Ni(II) for 40 mg L^{-1} concentration was studied as a function of pH from 2 to 8. The initial pH values were adjusted with Briton Robinson buffer solution containing 100 mg of an adsorbent. The contents were agitated for 60 min at 150 rpm, the suspensions were separated with an external magnet and the residual Ni(II) concentration was analyzed with atomic absorption spectroscopy (AAS). The effect of contact time at 150 rpm was studied for different time intervals from 20–60 min with 40 mg L^{-1} Ni(II) concentration, 100 mg adsorbent and pH 7. For equilibration studies, the concentration of Ni(II) was varied from 20–220 mg L^{-1} for 60 min. The thermodynamic

parameters were determined by performing the adsorption experiments at different temperatures from 30°C to100°C with 10°C interval. For the determination of percent adsorption and adsorption capacity, the following two equations were used [25,26].

$$\text{Percent Adsorption of Ni(II)} = \frac{C_0 - C_e}{C_0} \times 100 \quad (1)$$

$$\text{Adsorption capacity}\left(q_e\right) = \left(C_0 - C_e\right)\frac{V}{m} \quad (2)$$

where C_0 and C_e are the initial and equilibrium concentration of Ni(II), q_e is the adsorption capacity in mg g^{-1}, V is the volume of Ni(II) in mL, m is the mass of adsorbent in gram. Different kinetic and isotherm models were applied to explain the process of adsorption. All the experimental studies were performed in triplicate and average results were reported.

3. Results and discussion

3.1. Characterization of adsorbent

The MNP-OP composite was characterized using surface area and SEM. The BET and BJH surface area of MNP-OP composite were found to be 40.98 and 376.76 m^2 g^{-1} respectively. The BJH pore volume was found 1.43 cc g^{-1} and pore size 129.02 Å.

For the identification of surface functional group, Fourier-transform infrared (FTIR) spectra of OP and MNP-OP composite were recorded (Fig. 1). The comparison of the FTIR spectrum of OP (Fig. 1a) and MNPs-OP (Fig. 1b) composite shows the appearance, disappearance, and shifting of some peaks. Band shifting from 3,327; 2,918; and 1645 cm^{-1} on OP to 3,334; 2,923; and 1,623 cm^{-1} on MNPs-OP corresponding to the bonded –OH groups (carboxylic acid, phenols, and alcohols), –CH stretching and –C=O stretching in carboxyl group indicates that the MNPs are successfully bonded to OP. The disappearance of peak at 1,730 cm^{-1} on MNP-OP composite (present in OP due to stretching vibration of non-ionic carboxyl group –COOH) shows the binding of Fe with the –OH of the carboxyl group. The strong band at 1,012 cm^{-1} in both OP and MNP-OP is due to $-OCH_3$ groups confirms the presence of lignin in OP. The peek for the Fe–O is around 540–548 cm^{-1}.

SEM micrograph of OP, MNP-OP composite, MNP-OP composite after adsorption of Ni(II) and SEM image MNP are presented in Fig. 2. Fig. 2a shows the porous surface morphology of (OP) with an average pore size of 20 μm. Fig. 2b presents the MNP-OP composite shows that (OP) is covered with MNP and all the MNP aggregated on the surface of OP. In Fig. 2c, the surface morphology of the MNP-OP composite after adsorption of Ni(II) shows that the surface of adsorbent flattened as compared to the adsorbent before Ni(II) adsorption. While the SEM image of MNP shows that the nanoparticles are successfully synthesized having a particle size between 10–100 nm.

3.2. Effect of pH

In metal ion adsorption study, hydrogen ion concentration is an important parameter that affects the metal ion adsorption in solution. pH effect on % adsorption of Ni(II) ions onto MNP-OP composite is shown in Fig. 3. It can be concluded from Fig. 3 that percent adsorption increased with an increase in pH value from pH 2 to pH 7 with about 54%–97% adsorption. The point of zero charge (pzc) of the MNP-OP composite was determined and found pH 6.0 [19]. At pH < pH_{pzc}, the MNP-OP composite is positively charged while at pH > pH_{pzc} the MNP-OP composite is negatively charged. The low values of percent adsorption at lower pH may be due to the competition of H^+ ions with Ni(II) ions and H^+ ions are adsorbed preferentially than the Ni(II) ions. An increase in pH values leads to a decrease in H^+ ions concentration and an increase in Ni(II) ions adsorption on MNP-OP composite. The adsorption of Ni(II) ions on MNP-OP composite is due to ion exchange mechanism with weakly acidic hydroxyl and carboxyl groups as well as due to protonation and deprotonation of Fe_3O_4 nanoparticles present on the surface of the adsorbent. The protonation and deprotonation of MNP-OP composite surface are as follows:

$$\text{Fe–O–(C=O)–(OH)}_n + H^+ \rightleftharpoons \text{Fe–O–(C=O)–(OH}_2^+)_n \quad (3)$$

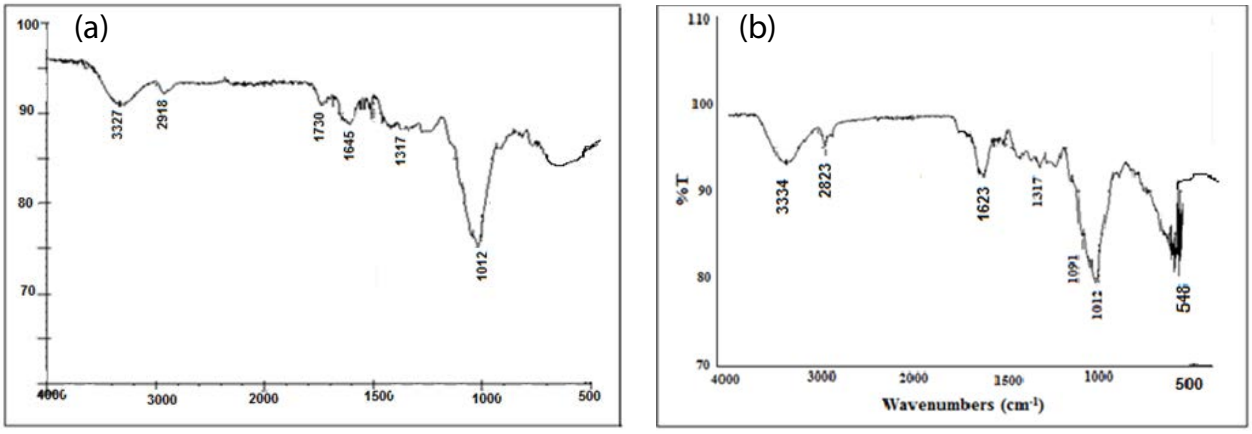

Fig. 1. FTIR spectra of (a) OP and (b) MNP-OP.

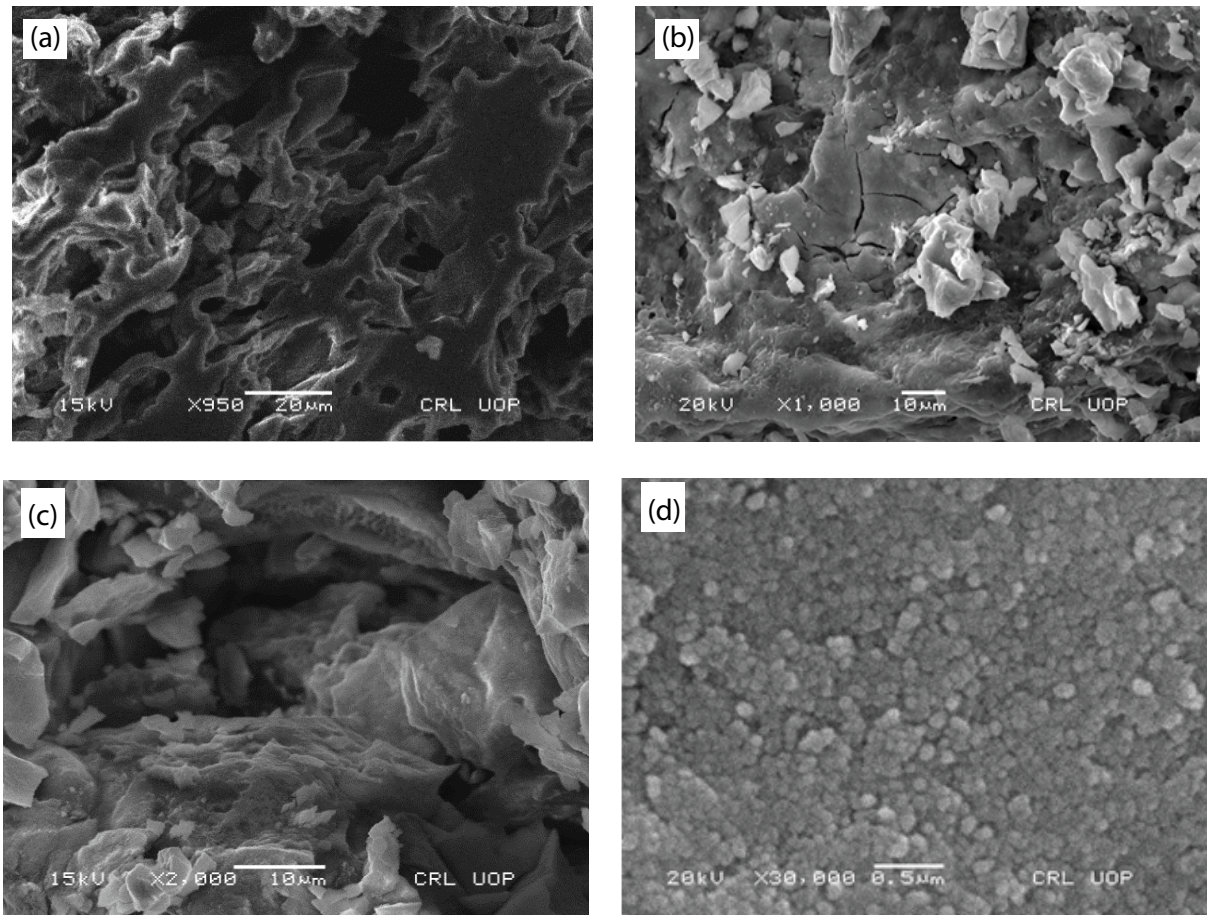

Fig. 2. SEM images of (a) OP, (b) MNP-OP, (c) MNP-OP after adsorption of Ni(II), and (d) MNP.

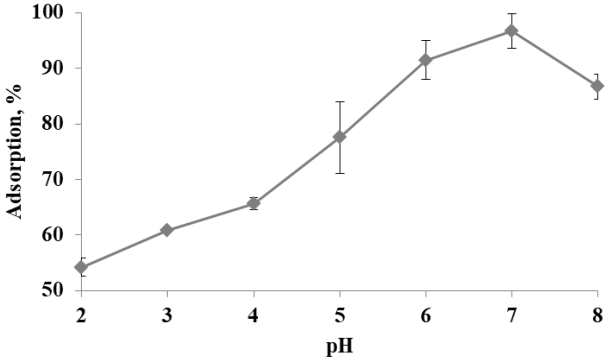

Fig. 3. Effect of pH on % adsorption of Ni(II) using MNP-OP as an adsorbent.

At lower pH –Fe–O–(C=O)–$(OH_2^+)_n$ is the predominant species and due to electrostatic repulsion between the positive charge adsorbent and Ni(II) occur which leads to decrease in adsorption of Ni(II) ions. At higher pH, the surface becomes negatively charge and –Fe–O–(C=O)–$(OH)_n$ is the dominant species. Electrostatic attraction between the deprotonated surface of adsorbent and Ni(II) ions results in increased adsorption. The adsorption process is mainly an ion-exchange and complexation process.

$$Fe–O–(C=O)–(OH)_n + Ni(II) \rightleftharpoons Fe–O–(C=O)–(O–Ni)_n^+ + nH^+ \quad (4)$$

3.2. Effect of amount of adsorbent

For the maximum interaction between sites of adsorbent and Ni(II) ions in solution, an optimum amount of adsorbent dose is required. Therefore, the effect of adsorbent dose on adsorption of Ni(II) ions on MNP-OP composite was studied in the range of 0.02–0.22 g and the results are shown in Fig. 4. The results showed that with an increase of adsorbent dose from 0.02 to 0.17 g; adsorption of Ni(II) also increased from 82.9% to 97.0%. There is no significant increase in the % adsorption of Ni(II) above 0.17 g of the adsorbent. This indicates that after a certain dosage of MNP-OP composite adsorbent, the maximum adsorption is obtained hence the amount of Ni(II) ions remains constant even with further increase in the adsorbent dosage, which further increases the available binding sites. Therefore further analyses were carried out with 0.17 g of MNP-OP composite as an adsorbent dosage.

3.3. Effect of agitation time

To observe the effect of agitation time on adsorption, it was varied from 15 to 120 min with a constant shaking speed of 150 rpm and the results are shown in Fig. 5.

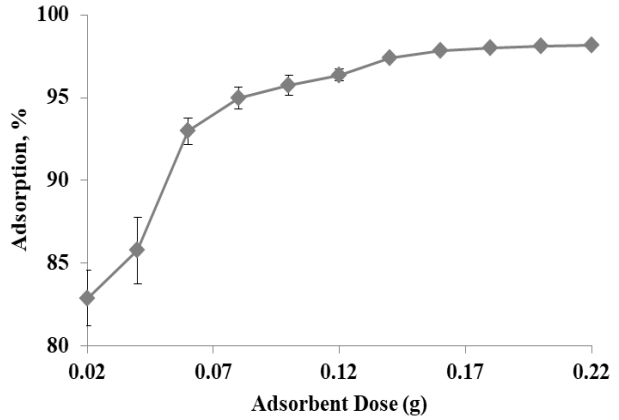

Fig. 4. Effect of adsorbent dose on % adsorption of Ni(II) as an adsorbent.

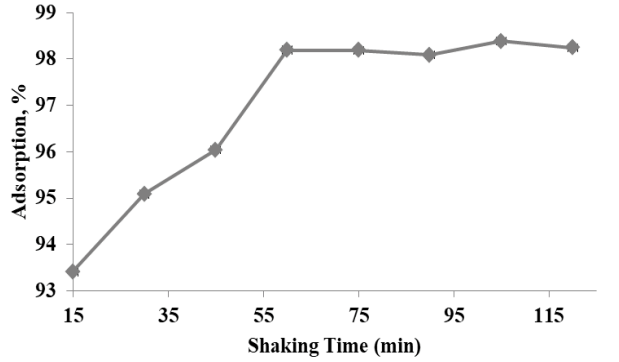

Fig. 5. Effect of agitation time on % adsorption of Ni(II) as an adsorbent.

The adsorption of Ni(II) ions is rapid in the beginning 15 min due to the free binding sites available on the MNP-OP composite. The equilibrium of percent adsorption reaches in 60 min for Ni(II) ions due to the used up of available binding sites and no pronounced effect was observed after 60 min.

3.4. Kinetic studies

To determine the rate constants, the kinetic data of Ni(II) adsorption on MNP-OP composite was evaluated by pseudo-first-order kinetics and pseudo-second-order kinetics. The mechanism of adsorption was evaluated by an intraparticle diffusion model. The following equation was used to express pseudo-second-order kinetics:

$$\log\left(q_e - q_t\right) = \log q_e - \frac{K_1 t}{2.303} \tag{5}$$

The values of equilibrium adsorption capacity (q_e), the rate constant for pseudo-first-order (K_1) and correlation coefficient (R^2) was calculated from the plot of pseudo-first-order kinetics (Fig. 6a) and are given in Table 1. The value of adsorption capacity (21.55 mg g^{-1}) calculated from the model is less than the experimental adsorption capacity (147.43 mg g^{-1}) value as well as the low value of R^2 (0.797).

Pseudo-second-order kinetics model can be expressed by the following equation:

$$\frac{t}{q_t} = \frac{t}{q_e} + \frac{1}{K_2 q_e^2} \tag{6}$$

The values of rate constant for pseudo-second-order kinetics (K_2) and equilibrium adsorption capacity (q_e) were calculated from the slope and intercept of the pseudo-second-order kinetic model (Fig. 6a and Table 1). The calculated adsorption capacity value (149.25 mg g^{-1}) is closer to the experimental adsorption capacity value (147.43 mg g^{-1}) with a high correlation co-coefficient (R^2 = 0.999). Therefore the data follows the pseudo-second-order kinetic equation (Table 1). Similar results have been reported in the literature [27,28].

For the evaluation of adsorption mechanism, Intraparticle diffusion model was applied and the following equation was used:

$$q_t = K_{\text{int}} t^{\frac{1}{2}} + C \tag{7}$$

where q_t is the sorption capacity at time t, K_{int} is the intraparticle diffusion rate constant, t is the time (min) (Fig. 6b). The figure shows that the adsorption plot is not linear over the whole time range studied and can be separated into two linear regions which confirm the multistage of adsorption. The first part signified that the Ni(II) ions were transported to the external surface of the MNP-OP composite through film diffusion and its rate was rapid. It may conclude from the figure that none of the plots gives a linear straight line segment passing through the origin. It indicates that some other mechanism such as ion exchange or complexation may also control the rate of adsorption along with the film diffusion process.

3.5. Isotherms studies

Adsorption isotherms were applied to analyze the maximum adsorption capacity of MNP-OP composite as

Table 1
Kinetic parameter of the adsorption of Ni(II) on the surface of MNP-OP

Metal ion	Experimental	Kinetic models								
		Pseudo-first-order			Pseudo-second-order			Intra particle diffusion		
	q_e mg g^{-1}	K_1 min^{-1}	q_e μg g^{-1}	R^2	K_2 min^{-1}	q_e μg g^{-1}	R^2	K_{int} min^{-1}	C	R^2
Ni(II)	147.428	0.060	21.550	0.797	0.006	149.250	0.999	0.030	137.370	0.834

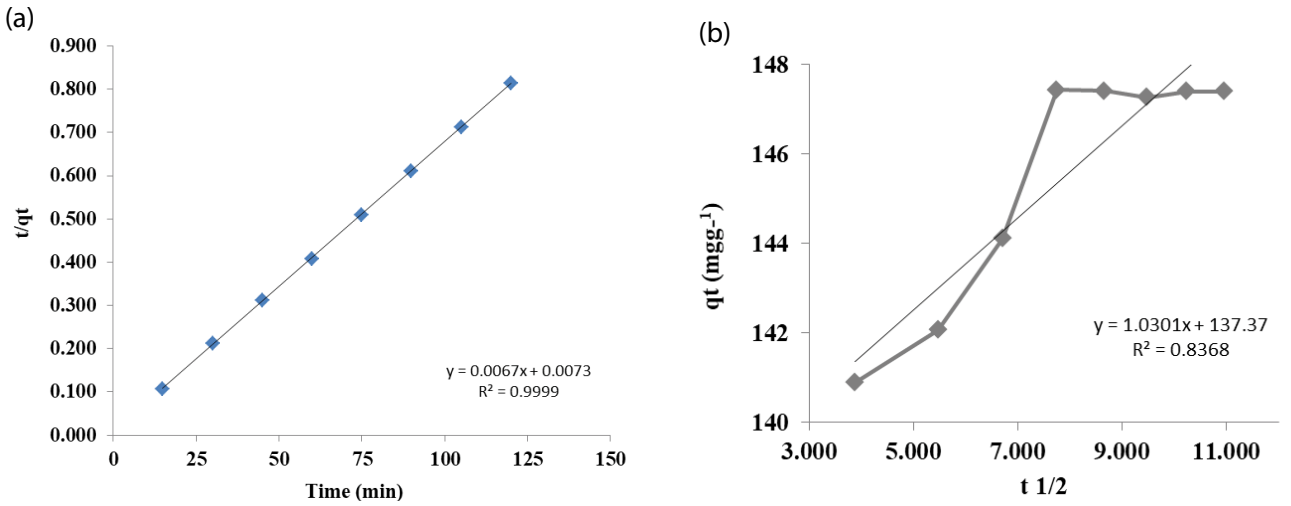

Fig. 6a. Pseudo-second-order kinetics model for adsorption of Ni(II) as an adsorbent.(b) Intraparticle diffusion model for adsorption of Ni(II) as an adsorbent.

an adsorbent for Ni(II). Langmuir and Freundlich isotherm models were applied. The parameter of these isotherms expresses the surface characteristics and the affinity of adsorbent towards adsorbate.

Langmuir adsorption isotherm was applied for the adsorption of Ni(II) on the MNP-OP composite. This adsorption isotherm is applicable for monolayer adsorption on homogenous surfaces within the MNP-OP composite. The linear form of the Langmuir isotherm is given as:

$$\frac{C_e}{q_e} = \frac{1}{K_L} + \frac{a_L C_e}{K_L} \tag{8}$$

where q_e is the adsorption capacity in (mg g^{-1}), C_e is the equilibrium concentration of the metal ion in (mg L^{-1}), a_L and K_L are Langmuir constant related to the adsorption energy and adsorbate–adsorbent binding force respectively. The plot of C_e/q_e to the C_e is a straight line and is shown in Fig. 7a. The high value of the correlation coefficient (R^2 = 0.9954) revealed that the equilibrium data fitted well to the experimental data by this model with adsorption capacity ($Q°$) of 110.12 mg g^{-1} (Table 2). The same results for Ni(II) adsorption have been reported in the literature [3,16].

The adsorption of the metal ions on the heterogeneous surface can be explained by using Freundlich adsorption isotherm, which is express by the following linear equation:

$$\log q_e = \log k_F + \frac{1}{n}\log C_e \tag{9}$$

where K_F is the relative adsorption capacity and $1/n$ indicates the intensity of the adsorption process. The plot between log q_e and log C_e gives a straight line as shown in Fig. 7b. The value of $1/n$ and K_F were calculated from the slope and intercept and given in Table 2. The value of n lies in between 1 and 10 indicate that the adsorption process is favorable with relatively good value of correlation coefficient (R^2 = 0.9750).

3.6. Thermodynamic studies

Effect of temperature on percent adsorption of Ni(II) onto MNP-OP composite was studied in the range from 303 to 363 K. The results revealed (Fig. 8) that an increase in adsorption occurred with an increase in temperature. The reason may be the availability of adsorption sites at high temperatures and desolvation of the species. High temperature also

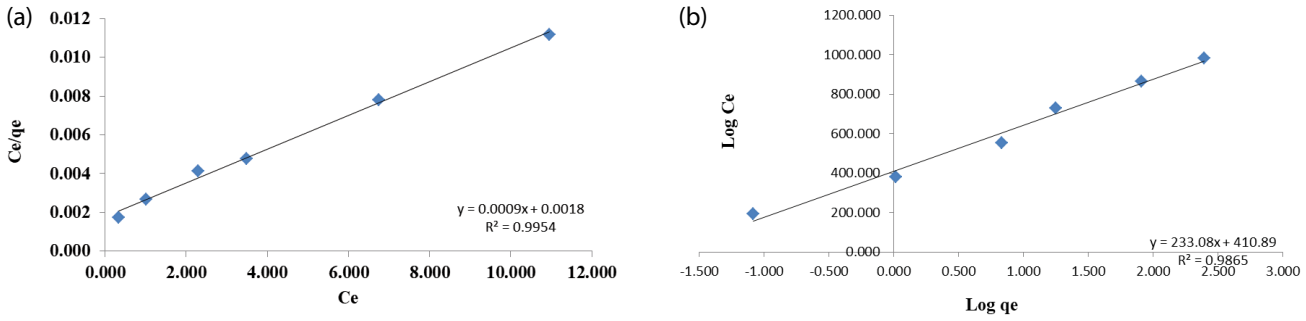

Fig. 7. (a) Langmuir adsorption isotherm for adsorption of Ni(II) using MNP-OP as an adsorbent, and (b) Freundlich adsorption isotherm for adsorption of Ni(II) using MNP-OP as an adsorbent.

Table 2
Comparison of different isotherm parameters

Adsorbent	Isotherm model							
	Freundlich				Langmuir			
	K_F (mg g^{-1})	n	$1/n$	R^2	K_L (L g^{-1})	a_L (L mg^{-1})	$Q°$ (mg g^{-1})	R^2
Ni(II)	100.620	2.120	0.471	0.975	555.550	0.500	110.120	0.995

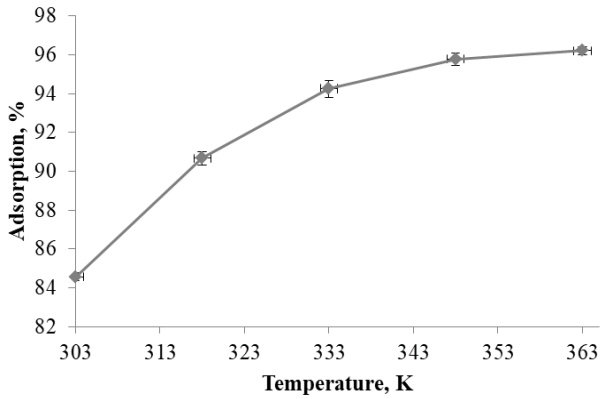

Fig. 8. Effect of temperature ions on % adsorption of Ni(II) using MNP-OP as an adsorbent.

leads to increased mobility of the Ni(II) ions and an increase in a collision between Ni(II) ions and MNP-OP composite adsorbent. It shows that high temperature favors the uptake of Ni(II) onto MNP-OP composite which indicated that the adsorption process is endothermic.

Thermodynamic parameters, that is, $\Delta H°$, $\Delta S°$, and $\Delta G°$ were determined using the Van't Hoff equation. The basic thermodynamic equations used are as:

$$K_D = \frac{q_e}{C_e} \tag{10}$$

$$\Delta G^0 = -\mathrm{RT}\ \ln \mathrm{k}_D \tag{11}$$

$$\ln K_D = \frac{\Delta S^0}{R} - \frac{\Delta H^0}{\mathrm{RT}} \tag{12}$$

where K_D is the equilibrium constant, q_e and C_e are the equilibrium concentration of the metal ion on the adsorbent (mg L^{-1}) and the concentration of the metal ion in the solution (mg L^{-1}) respectively. An increase in the K_D value with an increase in temperature shows that the adsorption process is endothermic. The positive values of ($\Delta S°$) and ($\Delta H°$) in Table 3 also show that the process is endothermic. The decrease in $\Delta G°$ values with an increase in temperature reveals that the adsorption of Ni(II) on to MNP-OP composite becomes better at a higher temperature. The positive value of $\Delta S°$ for the adsorption process indicated that there was an increase in randomness at the adsorbent-solution interface during the adsorption of the Ni(II) ions on the adsorbent sites, therefore, suggesting good affinity of Ni(II) on to MNP-OP composite adsorbent.

3.6. Effect of coexisting cations

The effect of different coexisting cations K^+, Na^+, Ca^{2+}, Mg^{2+}, Cr^{3+}, Cu^{2+} was studied on the adsorption of Ni(II) on the MNP-OP composite (Fig. 9). Wastewater contains different cations and it is important to study the competitive adsorption of these coexisting cations. As can be seen from the results that divalent metal ions affected the adsorption capacity of Ni(II), and decreased the adsorption capacity with an increase in the concentration of divalent metal ions from 1,000 to 2,000 μg which may be due to competitive adsorption of divalent metal ions for the sites on MNP-OP composite adsorbent. The competitive adsorptions generally vary with change in metal ion and depend on ion charges, molar mass, hydration energy of metal ion and ionic radii of hydrated metal ions.

3.7. Application to the real sample

The proposed adsorption method was applied for the removal of Ni(II) from real water samples collected from various areas of Pakistan. The water sample (10 mL) was taken, spiked with a known amount of Ni(II) and the removal efficiency of Ni(II) was determined. The removal efficiency of Ni(II) in all types of water studied varies from 97.91% to

Table 3
Thermodynamic parameters for the adsorption of Ni(II) on to MNP-OP

Temperature (K)	ln K_D	$\Delta G°$ (KJ mol^{-1})	$\Delta H°$ (KJ mol^{-1})	$\Delta S°$ (KJ mol^{-1})
303	3.716	–9.392		
318	4.294	–11.390		
333	4.842	–13.450	24.191	0.112
348	5.145	–14.933		
363	5.251	–15.900		

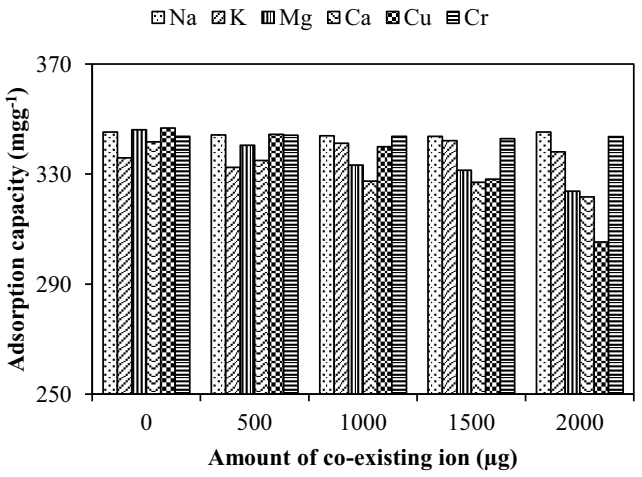

Fig. 9. Effect of coexisting ions on % adsorption of Ni(II) using MNP-OP as an adsorbent.

Table 4
Application of the proposed method for the removal of Ni(II) from various water samples (pH: 7, adsorbent dose: 0.1 g, equilibrium time: 60 min) $N = 3$

	Ni(II)		
Sample	Added (µg)	Adsorbed (µg)	Adsorption (%)
Tap water	100	100 ± 1	100
	300	297 ± 3	99
	500	480 ± 8	96
Canal water	100	98 ± 2	98
	300	294 ± 5	98
	500	485 ± 4	97
River water	100	99 ± 3	99
	300	297 ± 2	99
	500	490 ± 9	98

99.68% which shows that the effect of the coexisting metal ion is negligible (Table 4).

The method was compared with other solid phase extraction method in the literature using the value of adsorption capacity (Table 5). It can be concluded that the adsorbent used in this method is far better in its adsorption capacity as compared to other adsorbents.

4. Conclusion

In the present work waste MNP-OP and used for the removal of Ni(II) from water samples. Results indicated that the adsorption of Ni(II) on MNP-OP depends on pH and maximum Ni(II) was achieved at pH 7. The kinetic models show that the data fitted to the pseudo-second-order kinetic model because the experimental adsorption capacity q_e (147.428 mg g^{-1}) is closed to the calculated adsorption capacity q_e (149.250 mm g^{-1}) from pseudo-second-order kinetic. The adsorption isotherm was best described by the Langmuir adsorption isotherm with a high coefficient value of 0.995. The results of thermodynamic parameters showed that the adsorption of Ni(II) on MNP-OP is spontaneous and endothermic. The effect of coexisting metal ions was studied which showed that the presence of divalent metal ions had no significant effect on the removal efficiency of Ni(II) from aqueous solution. The most promising advantages of the prepared MNP-OP adsorbent are high surface area, environment-friendly and separation convenience with an external magnet from aqueous solutions.

Table 5
Comparison of the developed method with other adsorption methods

Method	Analysis	Adsorption capacity (q_e), mg g^{-1}	References
Solid phase extraction	AAS	Pb(II) = 45.0 Cd(II) = 45.0 Ni(II) = 43.2	[30]
Solid phase extraction	ICP-OES	Cr(III) = 39.85 Fe(III) = 29.69 Pb(II) = 54.48	[31]
Solid phase extraction	AAS	Cr(VI) = 9.50	[32]
Solid phase extraction	AAS	Cu(II) = 4.5 Ni(II) = 4.0 Zn(II) = 2.0	[33]
Solid phase extraction	AAS	Ni(II) = 147.5	This work

References

[1] P. Panneerselvam, N. Morad, KA. Tan, Magnetic nanoparticle (Fe_3O_4) impregnated onto tea waste for the removal of nickel(II) from aqueous solution, J. Hazard. Mater., 186, (2011) 160–168.
[2] M. Khan, M. Soylak, Magnetic solid phase extraction of lead, cadmium, and cobalt on magnetic carboxyl-modified nanodiamonds (MCNDS) from natural water samples and their determination by flame atomic absorption spectrometry, At. Spectrosc., 39 (2018) 81–89.
[3] J. Shah, M.R. Jan, A.U. Haq, M. Zeeshan, Equilibrium, kinetic and thermodynamic studies for sorption of Ni (II) from aqueous solution using formaldehyde treated waste tea leaves, J. Saudi Chem. Soc., 19 (2015) 301–310.
[4] P.K. Pandey, S. Choubey, Y. Verma, M. Pandey, S.S.K. Kamal, K. Chandrashekhar, Biosorptive removal of Ni(II) from wastewater and industrial effluent, Int. J. Environ. Res., 4 (2007) 332–339.
[5] E. Malkoc, Y. Nuhoglu, Investigations of nickel(II) removal from aqueous solutions using tea factory waste, J. Hazard. Mater., 127 (2005) 120–128.
[6] M. Khan, J. Shah, M.R. Jan, Magnetic solid phase extraction of Cd (II) using magnetic nanoparticle (MNPs) and silica coated magnetic nanoparticles (SiMNPs) from environmental water samples, Desal. Wat. Treat., 83 (2017) 123–132.
[7] Y. Iqbal, R. Ullah, M. Khan, Solid phase extraction of Pb(II) and Cd(II) using reduced graphene oxide-polychloroprene impregnated with magnetic nanoparticle (MNPs-RGO-PCP), Desal. Wat. Treat., 114 (2018) 232–241.
[8] M. Sadia, M.R. Jan, J. Shah, G.M. Greenway, Simultaneous preconcentration and determination of nickel and cobalt using functionalised mesoporous silica spheres by ICP-OES, Int. J. Environ. Res., 93 (2013) 1537–1556.

[9] M.E. Argun, S. Dursun, M. Karatas, Removal of Cd(II), Pb(II), Cu(II) and Ni(II) from water using modified pine bark, Desalination, 249 (2009) 519–527.
[10] M. Rafatullah, O. Sulaiman, R. Hashim, A. Ahmad, Adsorption of copper (II), chromium (III), nickel (II) and lead (II) ions from aqueous solutions by meranti sawdust, J. Hazard. Mater., 170 (2009) 969–977.
[11] W. Ma, J.M. Tobin, Development of multimetal binding model and application to binary metal biosorption onto peat biomass, Water Res., 37 (2003) 3967–3977.
[12] S. Kalyani, P.S. Rao, A. Krishnaiah, Removal of nickel (II) from aqueous solutions using marine macroalgae as the sorbing biomass, Chemosphere, 57 (2004) 1225–1229.
[13] V.K. Gupta, C.K. Jain, I. Ali, M. Sharma, V.K. Saini, Removal of cadmium and nickel from wastewater using bagasse fly ash—a sugar industry waste, Water Res., 37 (2003) 4038–4044.
[14] V. Padmavathy, Biosorption of nickel(II) ions by baker's yeast: kinetic, thermodynamic and desorption studies, Bioresour. Technol., 99 (2008) 3100–3109.
[15] H. Hasar, Adsorption of nickel(II) from aqueous solution onto activated carbon prepared from almond husk, J. Hazard. Mater., 97 (2005) 49–57.
[16] J. Shah, M.R. Jan, A.U. Haq, M. Sadia, Adsorptive removal of Ni (II) from aqueous solutions using carbon derived from mulberry wood sawdust, J. Chem. Soc. Pak., 34 (2012) 58–66.
[17] K. Vijayaraghavan, J. Jegan, K. Palanivelu, M. Velan, Biosorption of cobalt(II) and nickel(II) by seaweeds: batch and column studies, Sep. Purif. Technol., 44 (2005) 53–59.
[18] M. Khan, E. Yilmaz, M. Soylak, Vortex assisted magnetic solid phase extraction of lead(II) and cobalt(II) on silica coated magnetic multiwalled carbon nanotubes impregnated with 1-(2-pyridylazo)-2-naphthol, J. Mol. Liq., 224 (2016) 639–647.
[19] M. Khan, E. Yilmaz, B. Sevinc, E. Sahmetlioglu, J. Shah, M.R. Jan, M. Soylak, Preparation and characterization of magnetic allylamine modified graphene oxide-poly(vinyl acetate-co-divinylbenzene) nanocomposite for vortex assisted magnetic solid phase extraction of some metal ions, Talanta, 146 (2016) 130–137.
[20] Z.F. Wang, P.F. Xiao, N.Y. He, Synthesis and characteristics of carbon encapsulated magnetic nanoparticles produced by a hydrothermal reaction, Carbon, 44 (2006) 3277–3284.
[21] W.Y. William, J.C. Falkner, C.T. Yavuz, V.L. Colvin, Synthesis of monodisperse iron oxide nanocrystals by thermal decomposition of iron carboxylate salts, Chem. Commun., 20 (2004) 2306–2307.
[22] Y.-H. Deng, C.-C. Wang, J.-H. Hu, W.-L. Yang, S.-K. Fu, Investigation of formation of silica-coated magnetite nanoparticles via sol–gel approach, Colloids Surf., A, 262 (2005) 87–93.
[23] F. Grasset, N. Labhsetwar, D. Li, D.C. Park, N. Saito, H. Haneda, O. Cador, T. Roisnel, S. Mornet, E. Duguet, J. Portier, J. Etourneau, Synthesis and magnetic characterization of zinc ferrite nanoparticles with different environments: powder, colloidal solution, and zinc ferrite-silica core-shell nanoparticles, Langmuir, 18 (2002) 8209–8216.
[24] J. Shah, M.R. Jan, S. Jamil, A. ul Haq, Magnetic particles precipitated onto wheat husk for removal of methyl blue from aqueous solution, Toxicol. Environ. Chem., 96 (2014) 218–226.
[25] J. Shah, M.R. Jan, A.U. Haq, Y. Khan, Removal of Rhodamine B from aqueous solutions and wastewater by walnut shells: kinetics, equilibrium and thermodynamics studies, Front. Chem. Sci. Eng., 7 (2013) 428–436.
[26] J. Shah, M.R. Jan, M. Khan, S. Amir, Removal and recovery of cadmium from aqueous solutions using magnetic nanoparticle-modified sawdust: kinetics and adsorption isotherm studies, Desal. Wat. Treat., 57 (2016) 9736–9744.
[27] Y. Vijaya, S.R. Popuri, V.M. Boddu, A. Krishnaiah, Modified chitosan and calcium alginate biopolymer sorbents for removal of nickel (II) through adsorption, Carbohydr. Polym., 72 (2008) 261–271.
[28] Z. Chen, W. Ma, M. Han, Biosorption of nickel and copper onto treated alga (*Undaria pinnatifida*): application of isotherm and kinetic models, J. Hazard. Mater., 155 (2008) 327–333.
[29] A.-F. Ngomsik, A. Bee, J.-M. Siaugue, V. Cabuil, G. Cote, Nickel adsorption by magnetic alginate microcapsules containing an extractant, Water Res., 40 (2006) 1848–1856.
[30] Z.A. Alothman, E. Yilmaz, M. Habila, M. Soylak, Solid phase extraction of metal ions in environmental samples on 1-(2-pyridylazo)-2-naphthol impregnated activated carbon cloth, Ecotoxicol. Environ. Saf., 112 (2015) 74–79.
[31] Z.P. Zang, Z. Hu, Z.H. Li, Q. He, X.J. Chang, Synthesis, characterization and application of ethylenediamine-modified multiwalled carbon nanotubes for selective solid-phase extraction and preconcentration of metal ions, J. Hazard. Mater., 112 (2009) 958–963.
[32] M. Tuzen, M. Soylak, Multiwalled carbon nanotubes for speciation of chromium in environmental samples, J. Hazard. Mater., 147 (2007) 219–225.
[33] D. Božić, M. Gorgievski, V. Stanković, N. Štrbac, S. Šerbula, N. Petrović, Adsorption of heavy metal ions by beech sawdust – Kinetics, mechanism and equilibrium of the process, Ecol. Eng., 58 (2013) 202–206.